

ANNALI DELLA
SCUOLA NORMALE SUPERIORE DI PISA
Classe di Scienze

ROBERT A. HUMMEL

The hodograph method for convex profiles

Annali della Scuola Normale Superiore di Pisa, Classe di Scienze 4^e série, tome 9, n° 3
(1982), p. 341-364

http://www.numdam.org/item?id=ASNSP_1982_4_9_3_341_0

© Scuola Normale Superiore, Pisa, 1982, tous droits réservés.

L'accès aux archives de la revue « Annali della Scuola Normale Superiore di Pisa, Classe di Scienze » (<http://www.sns.it/it/edizioni/riviste/annaliscienze/>) implique l'accord avec les conditions générales d'utilisation (<http://www.numdam.org/conditions>). Toute utilisation commerciale ou impression systématique est constitutive d'une infraction pénale. Toute copie ou impression de ce fichier doit contenir la présente mention de copyright.

NUMDAM

Article numérisé dans le cadre du programme
Numérisation de documents anciens mathématiques
<http://www.numdam.org/>

The Hodograph Method for Convex Profiles.

ROBERT A. HUMMEL (*)

1. - Introduction.

This paper extends results of Brezis and Stampacchia [1] concerning the problem of planar fluid flow past a given profile with prescribed velocity at infinity. Brezis and Stampacchia showed that the hodograph method for this classical problem warrants reconsideration using variational inequalities. Their treatment is restricted to symmetric planar flow past an obstacle which is convex and symmetric with respect to the horizontal axis. In this paper we treat flows with zero circulation past strictly convex, but not necessarily symmetric, obstacles.

One of the principal advantages of the hodograph method is that the nonlinear compressible fluid flow equation becomes linear in the hodograph domain. The variational inequality posed in the hodograph domain for a symmetric profile and incompressible fluid, as described in [1], has been extended to treat compressible fluid flow past a symmetric obstacle [2]. Although we restrict the analysis to incompressible fluids in this paper, a similar extension to compressible flow past convex obstacles is possible (to be treated later). Extensions to flow in a channel [3], and flows with cavitation [4] have been investigated for the symmetric profile case. Analogs of these extensions in the case of a general convex profile may be possible, but are not considered here.

For convex, symmetric profiles, Brezis and Stampacchia showed that the symmetric flow solution can be obtained from the solution to a variational inequality, or from the solution to a certain minimization problem. The domain of the class of competing functions in these problems is the hodograph image of the portion of the flow region above the axis of symmetry. The solution may be viewed as the projection of a certain function

(*) Supported in part by U. S. Army Research Office Grant Number DAAG29-81-K-0043 and NSF-MCS-79-00813, with the National Science Foundation.

Pervenuto alla Redazione il 29 Aprile 1981 ed in forma definitiva il 30 Novembre 1981.

onto a convex set in the Sobolev space H_0^1 of functions defined on a modified hodograph plane.

In the extension to convex, nonsymmetric profiles, the entire hodograph image must be used, and is most conveniently viewed as a Riemann surface. We show in Section 3 that the Riemann surface Ω always has two sheets with a single, known, branch point. The class of competing functions with domain Ω can then be defined, and the results of Brezis and Stampacchia may be extended to the new class. In Section 4 we show that this extension leads to a quasi-variational inequality for the flow solution. Finally, in Section 5, we pose a variational inequality. In this inequality, the class of competing functions is a convex set of functions defined on Ω , positive on one of the sheets and negative on the other sheet, with a specified jump across a pair of cut lines. The profile geometry is used to define a distribution T on the Riemann surface, and a symmetric bilinear form $a(u, v)$ for functions in $H_0^1(\Omega)$ is also given. The variational inequality will take the form:

$$\text{Find } u \in \mathbf{K}: a(u, v - u) \geq \langle T, v - u \rangle \quad \text{for all } v \in \mathbf{K}.$$

We will then show that the flow solution may be obtained easily from $\text{grad } u$.

Throughout, we consider incompressible, irrotational, inviscid, steady planar fluid flow past an obstacle. The equations of motion are derived from the equation of continuity, and the irrotationality condition. For general bounded obstacles, the classical existence and uniqueness theory for flows with prescribed circulation is equivalent to applying the Riemann mapping theorem to determine conformal maps. It should be emphasized that a solution is possible for any prescribed circulation, which is tantamount to prescribing the total lift on the obstacle. The question of determining the physically stable, or naturally occurring circulation cannot be addressed without imposing additional constraints. In this paper, we seek the no-lift solution, which requires that the circulation about the profile be zero. Although the no-lift solution may not be the most desirable solution, the general solution for any nonzero circulation can be obtained from the zero circulation flow. The formulation of a variational inequality in the hodograph domain is facilitated by the zero circulation requirement.

We assume that the prescribed velocity at infinity is sufficiently small that no cavitation takes place in the flow region. We will also assume that the profile is smooth (at least $C^{2,\alpha}$), since the presence of cusps or singularities on the profile boundary give rise to singularities in the flow solution, or can be interpreted as requiring a particular circulation so that the flow will be continuous. In the symmetric case, corners are allowed at the leading

and trailing edges because it is known a priori that the stagnation points will occur there. For convex profiles, the determination of the stagnation points is part of the solution.

The results of this paper were obtained as part of the author's Ph. D. thesis at the University of Minnesota, 1980. The author gratefully acknowledges the kind assistance and encouragement of his advisor, David Kinderlehrer.

2. - Formulation in the physical plane.

To formulate the planar flow problem past a bounded convex obstacle, we assume we are given a closed, bounded, strictly convex subset \mathfrak{F} of the complex plane. Further, we assume that $\partial\mathfrak{F}$ is $C^{2,\alpha}$ ($0 < \alpha < 1$), and that the flow velocity q_∞ at infinity is given, with $q_\infty > 0$. The flow region $C \setminus \mathfrak{F}$ will be denoted by G .

At any point $z \in G$, the associated flow velocity vector is $\bar{q} = (q_1(z), q_2(z))$. The flow problem is given by

$$(2.1) \quad \text{Find } \bar{q}(z) = (q_1, q_2) \quad \text{satisfying}$$

- i) $q_1(z), q_2(z) \in C^1(G) \cap C^0(\bar{G})$;
- ii) $\operatorname{div} \bar{q} = 0$ in G ;
- iii) $\operatorname{curl} \bar{q} = 0$ in G ;
- iv) $\bar{q}(z) \cdot \bar{n} = 0$ for $z \in \partial G$,
where \bar{n} = normal to ∂G at z ;
- v) $\bar{q}(z) \rightarrow (q_\infty, 0)$ as $z \rightarrow \infty$.

For any solution to (i)-(v), the circulation about \mathfrak{F} is defined by

$$\Gamma = \oint_{\partial\mathfrak{F}} q_1 dx + q_2 dy.$$

There is a one-parameter family of solutions to (i)-(v), parameterized by the circulation Γ , which in turn is directly proportional to the lift on the profile. We seek the no-lift solution, which is prescribed by the side condition

$$(2.1) \text{ vi) } \quad \Gamma = 0.$$

For any given value Γ , there is a unique flow satisfying (i)-(v) whose circulation is the prescribed value Γ . This solution may be constructed as follows:

Let $f(z)$ be the conformal map taking G onto $\{z: |z| > 1\}$, with $f(\infty) = \infty$ and $f'(\infty) > 0$. Then let

$$\Phi(z) = \frac{q_\infty}{f'(\infty)} \left(f(z) + \frac{1}{f(z)} \right) - \frac{i\Gamma}{2\pi} \log f(z),$$

and

$$V(z) = \Phi'(z) = q_1(z) - iq_2(z)$$

where

$$q_1(z), \quad q_2(z) \in \mathbf{R}.$$

Then $\bar{q} = (q_1, q_2)$ is the desired solution. In particular, the problem (i)-(vi) has a unique solution which may be constructed from the conformal map $f(z)$, by setting $\Gamma = 0$.

In this paper, we seek an alternate construction of the solution to the problem (i)-(vi). The method will apply only to convex profiles, and requires the condition $\Gamma = 0$. However, the new algorithm will replace the use of the Riemann mapping theorem with the construction of a solution to a variational inequality. Further, the new method extends quite easily to compressible fluids. The notation defined below will be used in the construction.

In general, any solution \bar{q} to (i)-(v) defines a function

$$V(z) = q_1(z) - iq_2(z)$$

which extends to a holomorphic function in $G \cup \{\infty\}$. A possibly multi-valued primitive $\Phi(z)$ always exists, so that

$$(2.2) \quad \Phi'(z) = V(z) \quad \text{and} \quad \Phi(z) = \varphi(z) + i\psi(z).$$

The harmonic functions $\varphi(z)$ and $\psi(z)$ are the potential and stream functions respectively. In light of condition (iv), the stream function is always single valued. Further, the stream function is constant on stream lines, and thus constant on $\partial\mathcal{F}$. We may assume without loss of generality that

$$(2.3) \quad \psi(z) \equiv 0 \quad \text{on} \quad \partial\mathcal{F}.$$

Note that the stream function satisfies

$$(2.4) \quad \frac{\partial\psi}{\partial x} = -q_2, \quad \frac{\partial\psi}{\partial y} = q_1.$$

The convexity of the profile boundary is required in order to represent points on the boundary in terms of the tangent orientation. Since the flow direction at a boundary point is a tangent direction, this representation is extremely useful for hodograph methods. We define

$$Z_+(\theta) = X_+(\theta) + iY_+(\theta), \quad -\pi < \theta \leq \pi$$

to be the complex coordinate of the point on $\partial\mathcal{F}$ whose clockwise oriented tangent has argument θ . At $\theta = -\pi$, $Z_+(\theta)$ is located at the «lowermost point» of $\partial\mathcal{F}$, and processes in a counterclockwise direction once around $\partial\mathcal{F}$ as θ increases to π .

The counterclockwise oriented tangent can serve as a parameter as well as the clockwise oriented tangent. We define

$$Z_-(\theta) = X_-(\theta) + iY_-(\theta), \quad -\pi < \theta \leq \pi$$

to be the point of $\partial\mathcal{F}$ whose counterclockwise oriented tangent has argument θ . In this case, as θ increases from $-\pi$ to π , $Z_-(\theta)$ travels from the uppermost point of $\partial\mathcal{F}$ in a counterclockwise direction once around $\partial\mathcal{F}$. Since $Z_+(\theta)$ and $Z_-(\theta)$ describe the same curve, they are related by

$$(2.5) \quad \begin{cases} Z_-(\theta) = Z_+(\theta + \pi), & -\pi < \theta \leq 0 \\ Z_-(\theta) = Z_+(\theta - \pi), & 0 < \theta \leq \pi. \end{cases}$$

Despite these relations, it will be useful to retain both functions.

Although $\partial\mathcal{F}$ is $C^{2,\alpha}$, a derivative is lost in the representation of the boundary, and thus X_+ , X_- , Y_+ , and Y_- are $C^{1,\alpha}$ functions of θ . The tangent vectors $(X'_+(\theta), Y'_+(\theta))$ and $(X'_-(\theta), Y'_-(\theta))$ have arguments $\theta + \pi$ and θ respectively, and so are always perpendicular to the boundary normal $(\sin \theta, -\cos \theta)$. Thus

$$(2.6) \quad X'_\pm(\theta) \sin \theta - Y'_\pm(\theta) \cos \theta = 0, \quad \text{all } \theta,$$

either + or - subscript consistently.

The following notation will also be used. The total profile height is

$$(2.7) \quad H = Y_+(0) - Y_-(0),$$

and the horizontal displacement of the upper and lower extreme points is

$$(2.8) \quad W = X_+(0) - X_-(0).$$

Note that $W = 0$ for symmetric profiles. The curvature functions are given by

$$(2.9) \quad R_{\pm}(\theta) = X'_{\pm}(\theta) \cos \theta + Y'_{\pm}(\theta) \sin \theta .$$

Since $(X'_{+}(\theta), Y'_{+}(\theta))$ is a vector in the same direction as $-(\cos \theta, \sin \theta), -R_{+}(\theta)$ is simply the magnitude of the vector (X'_{+}, Y'_{+}) , i.e., $\sqrt{(X'_{+}(\theta))^2 + (Y'_{+}(\theta))^2}$, which is the curvature of $\partial\mathcal{F}$ at $(X_{+}(\theta), Y_{+}(\theta))$. Note that

$$(2.10a) \quad R_{+}(\theta) < 0, \quad \text{all } \theta .$$

Likewise, $(X'_{-}(\theta), Y'_{-}(\theta))$ lies in the same direction as $(\cos \theta, \sin \theta)$, and so

$$(2.10b) \quad R_{-}(\theta) > 0, \quad \text{all } \theta .$$

3. - The hodograph domain.

A hodograph transform replaces the physical coordinates of the flow region with coordinates formed by the components of velocity. If the transformation

$$(x, y) \rightarrow (q_1(x, y), q_2(x, y))$$

is locally one-to-one at a point, then the flow solution near that point can be represented by the inverse map, which is a function of the hodograph variables (q_1, q_2) .

In general, the hodograph transform (or equivalently, the map $z \rightarrow V(z)$) is not globally one-to-one. Accordingly, the desired inverse map, regarded as a function of the entire hodograph image, will be multivalued. One way to deal with this situation is to solve for the different branches of the inverse function separately. This is the approach used for symmetric obstacles in [1], and provides a solution because the two branches are related by the symmetry of the problem.

For nonsymmetric profiles, we will need to use all branches simultaneously. Since $V(z)$ is holomorphic, we can view the hodograph domain as a Riemann surface in one-to-one correspondence with the flow region. In this way, the hodograph domain becomes more complicated, but the inverse to the hodograph transformation is single-valued.

For convex profiles, it is possible to determine a-priori the general structure of the Riemann surface of the hodograph image. Briefly, we will show that the hodograph may be viewed as a two-sheeted surface lying

over a bounded region of the complex plane with a single first order branch point at q_∞ . The map $V(z)$ takes G onto the bounded region, conformally mapping an upper region G_+ onto a slit region, and conformally mapping a lower region G_- onto an overlapping region, slit along the same line (see Figure 3.1). The next lemma justifies this figure.

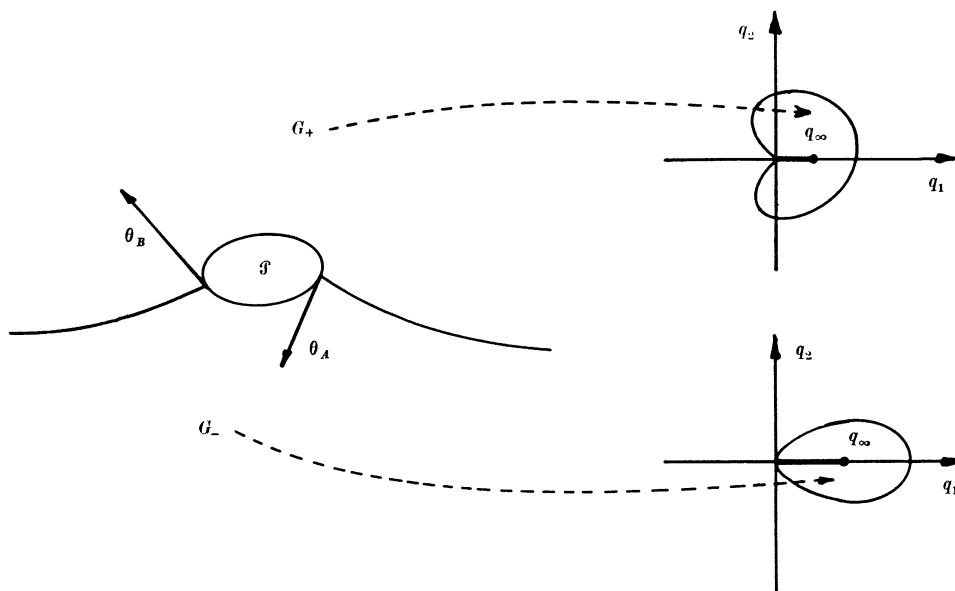


Figure 3.1. The hodograph transform.

LEMMA 3.1. *Assume that \mathcal{F} is strictly convex, and that $V(z)$ solves the flow problem (2.1), (i)-(vi).*

- (a) $V(\partial G)$ consists of two closed curves joined at 0. $V(z) = \zeta$ has at most two solutions for a given ζ .
- (b) $V'(z) = 0$ if and only if $z = \infty$.
- (c) There is a left stagnation point and a right stagnation point on the profile boundary. The flow travels from the left to the right stagnation point along both the upper and lower portions of the boundary.
- (d) $V(z) = \zeta$ has no solution for $\zeta < 0$, and two distinct solutions for $0 \leq \zeta < q_\infty$.
- (e) The set $G \setminus \{z: 0 \leq V(z) < q_\infty\}$ consists of two regions G_+ and G_- . $V(z)$ is one-to-one on G_+ and on G_- .

PROOF. Recall from the construction of the flow solution in Section 2 that when $I = 0$,

$$(3.1) \quad V(z) = \frac{q_\infty}{f'(\infty)} \cdot f'(z) \cdot \left(1 - \frac{1}{(f(z))^2} \right),$$

where $f(z)$ is the conformal map of G onto $\{z \in \mathbf{C}: |z| > 1\}$, with $f(\infty) = \infty$, and $f'(\infty) > 0$. Since $f(z)$ is conformal, $f'(z) \neq 0$ for $z \in G$. Thus $V(z) \neq 0$ in G . On ∂G , the same formula for $V(z)$ holds, but $f(z)$ and $f'(z)$ must be interpreted properly. The regularity of the boundary permits $f(z)$ to be extended to a homeomorphism of \bar{G} onto $\{|z| \geq 1\}$, by, say, Theorem 14.19 of [5]. To show that $f'(z)$ exists on ∂G , one must apply a theorem of Warschawski [6] to the inverse map of $f(z)$, which is a conformal map from $\{|z| > 1\}$ onto G . To satisfy the hypotheses of Warschawski's theorem, it suffices to show that the θ parameterization of ∂G as a function of arclength $\theta = \theta(s)$, is a Lipschitz function. However, since \mathfrak{F} is $C^{2,\alpha}$, $\theta = \theta(s)$ is a $C^{1,\alpha}$ function, and thus assuredly Lipschitz. We conclude from [6] that f^{-1} extends to be C^1 on $\{|z| \geq 1\}$, with nonzero derivative for $|z| = 1$. Accordingly $f(z)$ is likewise differentiable on ∂G , and $f'(z) \neq 0$ for $z \in \partial G$. Using (3.1), we see that $V(z) = 0$ only at those points in \bar{G} where $f(z) = 1$ or $f(z) = -1$. Consequently, there are exactly two stagnation points (solutions to $V(z) = 0$) in \bar{G} , both located on the profile boundary. These points can be denoted by $Z_+(\theta_A)$ and $Z_+(\theta_B)$, where $-\pi \leq \theta_A < \theta_B \leq \pi$.

For all θ except θ_A and θ_B ,

$$(3.2) \quad \arg \overline{V(Z_+(\theta))} = \theta, \quad \text{or } \theta + \pi$$

depending on whether the flow is directed in a clockwise or counterclockwise direction around $\partial \mathfrak{F}$. The profile boundary without the two stagnation points has two components. Along each component, the flow orientation must be consistent, since a change in orientation can only occur at a stagnation point. Thus the image under $\overline{V(z)}$ of each of the components consists of a curve emanating from 0, sweeping out points whose arguments vary from θ_A to θ_B (modulo 2π), or from $\theta_A + \pi$ to $\theta_B + \pi$. Since $\arg \overline{V(Z_+(\theta))}$ varies monotonically, each image forms a simple closed curve starting and returning to 0.

Next, since $V(z)$ is holomorphic in G , the number of solutions to $V(z) = \zeta$ equals the winding number of $V(\partial \mathfrak{F})$, properly oriented, about the point ζ . Because $V(\partial \mathfrak{F})$ consists of two simple closed curves, this winding number is at most two. This proves statement (a).

To prove (b), we first observe that $V(G)$ is bounded, since $V(\infty) = q_\infty$ is a removable singularity. This means that $V(G)$ consists of the interior

regions bounded by $V(\partial G)$. Suppose that the flow orientation is entirely clockwise or entirely counterclockwise around $\partial \mathcal{B}$. This in fact happens when the magnitude of Γ is large. When Γ is zero, this cannot happen, since then $\arg V(Z_+(\theta))$ would span the full circle from $-\pi$ to π as θ varies through its range from $-\pi$ to π (Equation (3.2)). This results in a disconnected image $V(G)$, since $V(Z_+(\theta))$ is pinched at the origin when $\theta = \theta_A$ and θ_B (see Figure 3.2). Thus the flow orientation must switch as one crosses a stagnation point.

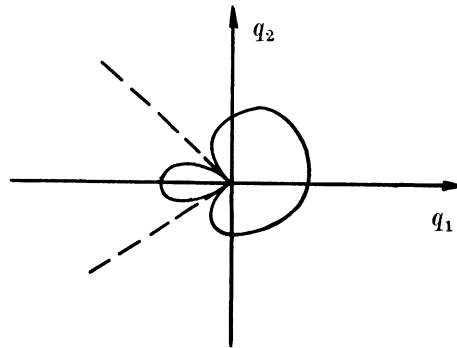


Figure 3.2

To count the number of zeros of $V'(z)$, note that the tangent to $V(\partial G)$ rotates twice as one travels once around $V(\partial G)$, according to the results above (see Figure 3.3). However, if $g(z)$ is any holomorphic map of a simply connected domain \mathcal{D} onto a bounded region, with $g(\partial \mathcal{D})$ a nonsimple closed curve which winds twice around an interior region, then $g'(z)$ must have exactly one zero in \mathcal{D} . This follows from the argument principle applied to $g'(z)$, where the winding number is calculated using a parameterization $z = u(t)$ of $\partial \mathcal{D}$. Specifically,

$$\frac{1}{2\pi} \Delta \arg g'(u(t)) = \frac{1}{2\pi} \Delta \arg \frac{d}{dt} (g(u(t))) - \frac{1}{2\pi} \Delta \arg u'(t) = 2 - 1 = 1.$$

Since $G \cup \{\infty\}$ can be viewed as a simply connected domain, $V'(z)$ must have one zero in $G \cup \{\infty\}$. But since $V(z) = q_\infty + a_{-2}/z^2 + \dots$ near ∞ (using $\Gamma = 0$), $V'(\infty) = 0$ is the unique zero of $V'(z)$. This proves part (b).

Next observe that $V(\infty) = q_\infty$ and $V'(\infty) = 0$ imply that $V(z) = q_\infty$ has at least two solutions, counting multiplicity. From part (a), q_∞ must be covered exactly twice, and so $V(\partial G)$ winds twice around q_∞ . Thus

$$V(Z_+(0)) > q_\infty \quad \text{and} \quad V(Z_+(\pi)) > q_\infty.$$

This says that the flow is to the right at both the uppermost and lowermost points of $\partial\mathcal{F}$. Since the flow orientation is opposite at these two points, there must be a stagnation point on the «right»

$$(3.3a) \quad z_A = Z_+(\theta_A), \quad \text{with} \quad -\pi < \theta_A < 0,$$

and another stagnation point on the «left»:

$$(3.3b) \quad z_B = Z_+(\theta_B), \quad \text{with} \quad 0 < \theta_B < \pi.$$

Part (c) follows.

On the upper portion of the profile, $Z_+(\theta)$ for $\theta_A < \theta < \theta_B$, the flow is clockwise, so that $\arg(q_1 + iq_2)$ is in the same direction as θ , and

$$(3.4a) \quad \arg \overline{V(Z_+(\theta))} = \theta, \quad \theta_A < \theta < \theta_B.$$

On the lower portion of the curve, the flow orientation is opposite, so

$$(3.4b) \quad \arg \overline{V(Z_+(\theta))} = \theta + \pi, \quad -\pi \leq \theta < \theta_A \quad \text{and} \quad \theta_B < \theta \leq \pi.$$

As θ varies from $-\pi$ to π , the curve $\overline{V(Z_+(\theta))}$ looks like Figure 3.3, winding twice around the segment $0 < \zeta < q_\infty$, and without crossing the negative real axis. The assertions of part (d) follow.

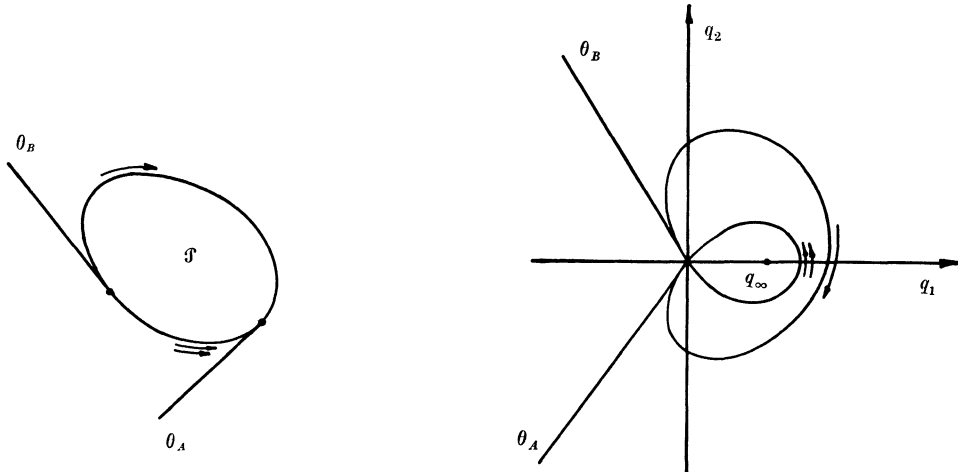


Figure 3.3

By lifting the map $V(z) = \zeta$ for $0 \leq \zeta \leq q_\infty$, we obtain two curves, each emanating from one of the stagnation points, and each terminating at $z = \infty$, which is the only solution to $V(z) = q_\infty$. The two curves intersect only at $z = \infty$, since q_∞ is the only point in $V(G)$ which is multiply covered by a single point in the physical domain. These curves separate \bar{G} into two components: one component, G_+ , contains the upper profile point $Z_+(0)$, the other component, G_- , contains the lowermost profile point $Z_-(0)$. The image of the boundary of G_+ consists of a simple closed curve together with the slit $0 \leq \zeta \leq q_\infty$ traversed twice. Thus $V(z)$ is univalent on G_+ , and likewise univalent on G_- . This completes the proof of Lemma 3.1.

Lemma 3.1 allows us to describe the Riemann surface associated with the hodograph domain. Clearly, $V(z)$ can be lifted to a univalent conformal map of G onto a double-sheeted branched Riemann surface. One sheet arises from the image of G_+ , and the other sheet from G_- . The point $\zeta = q_\infty$ is a first order branch point connecting the two sheets. The sheets are cut along the lines $0 \leq \zeta \leq q_\infty$, with upper and lower shores of the cut lines on opposite sheets associated, representing the continuous structure of the image of the physical domain as one crosses the lines $\{z \in G: 0 < V(z) < q_\infty\}$. One can view the hodograph domain as a subset of the Riemann surface of the equation $w = \sqrt{\zeta - q_\infty}$.

It is customary in hodograph methods to use the coordinates (θ, σ) defined by

$$\theta + i\sigma = -i \log \overline{V(z)}.$$

These coordinates on the hodograph surface are especially convenient because

$$\theta = \arg \overline{V(z)} = \arg(q_1 + iq_2),$$

while

$$\sigma = -\log |V(z)| = -\log |\bar{q}|.$$

Since $V(z)$ is never negative (Lemma 3.1 (d)), the transformation from the $\zeta = q_1 - iq_2$ coordinate to (θ, σ) coordinates is one-to-one on both sheets.

In (θ, σ) coordinates, the Riemann surface of the hodograph domain has a different shape (see Figure 3.4). There are two sheets, branched over the point $(0, \sigma_\infty)$, where $\sigma_\infty = -\log q_\infty$. The cut lines are transformed to the vertical straight lines $\theta = 0, \sigma \geq \sigma_\infty$ (on both sheets). One of the sheets is formed by the image of G_+ , and is given by

$$\mathcal{D}_+ = \{(\theta, \sigma): \sigma > l_+(\theta), \theta_A < \theta < \theta_B\} \setminus \{(0, \sigma): \sigma \geq \sigma_\infty\}$$

where $l_+(\theta) = -\log |V(Z_+(\theta))|$. Note that the domain of $l_+(\theta)$ is (θ_A, θ_B) , since $\arg \overline{V(z)}$ varies from θ_A to θ_B as z traverses the G_+ portion of $\partial\mathcal{F}$ (Equa-

tion (3.4a)). The other sheet is given by

$$\mathfrak{D}_- = \{(\theta, \sigma) : \sigma > l_-(\theta), \theta_B - \pi < \theta < \theta_A + \pi\} \setminus \{(0, \sigma) : \sigma \geq \sigma_\infty\}.$$

Here $l_-(\theta) = -\log |V(Z_-(\theta))|$, and the domain is $(\theta_B - \pi, \theta_A + \pi)$ according to equation (3.4b).

At $\theta = \theta_A$ and $\theta = \theta_B$, $V(Z_+(\theta)) = 0$, and so $l_+(\theta)$ has vertical asymptotes. Likewise, $l_-(\theta)$ has asymptotes at $\theta = \theta_B - \pi$ and $\theta = \theta_A + \pi$. We will denote the external boundary curves by

$$(3.5) \quad \Gamma_+ = \{(\theta, l_+(\theta)) : \theta_A < \theta < \theta_B\} \quad \text{and} \quad \Gamma_- = \{(\theta, l_-(\theta)) : \theta_B - \pi < \theta < \theta_A + \pi\}.$$

The cut lines arise from the image of the two curves $\{z : 0 \leq V(z) < q_\infty\}$, (Lemma 3.1e). One curve, joining the right stagnation point $Z_+(\theta_A)$ with $z = \infty$, transforms to a cut connecting $\theta < 0$ points on the \mathfrak{D}_+ sheet with $\theta > 0$ points on the \mathfrak{D}_- sheet. The other curve, which joins $Z_+(\theta_B)$ with $z = \infty$, is mapped to the cut connecting $\theta > 0$ points on the \mathfrak{D}_+ sheet with $\theta < 0$ points on the \mathfrak{D}_- sheet. We will denote the first cut, connecting the

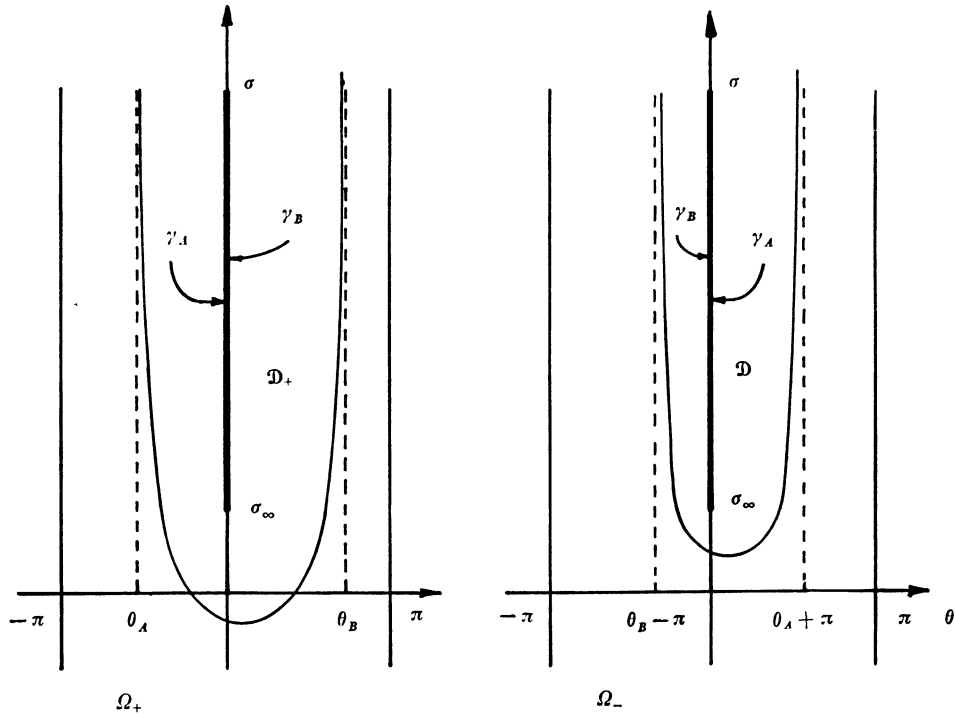


Figure 3.4

left shore on \mathfrak{D}_+ with the right shore on \mathfrak{D}_- , by γ_A . The other cut, identifying the right shore on \mathfrak{D}_+ with the left shore on \mathfrak{D}_- , will be denoted by γ_B . By including the point $(0, \sigma_\infty)$ as a first order branch point, we obtain a Riemann surface \mathfrak{D} .

Of course, the parameters controlling the location of the asymptotes, θ_A and θ_B , as well as the curves $\sigma = l_+(\theta)$ and $\sigma = l_-(\theta)$ are not known a-priori. They will be determined from the free boundary of a solution function whose domain is an extended hodograph surface. Specifically, since $-\pi \leq \theta_A < \theta_B \leq \pi$, \mathfrak{D}_+ is always contained in

$$\Omega_+ = \{(\theta, \sigma) : -\pi < \theta < \pi\} \setminus \{(0, \sigma) : \sigma \geq \sigma_\infty\};$$

and \mathfrak{D}_- is a subset of an identical copy of the set Ω_+ , which we denote by Ω_- . If we make the same identifications on the vertical cut lines as exist between \mathfrak{D}_+ and \mathfrak{D}_- , and include $(0, \sigma_\infty)$ as a first order branch point, we obtain a Riemann surface Ω which contains the (θ, σ) representation of the hodograph domain \mathfrak{D} (see Figure 3.4). The surface Ω is in fact the (θ, σ) representation of the Riemann surface $w = \sqrt{\zeta - q_\infty}$.

In summary, the map $\theta + i\sigma = -i \log \overline{V(z)}$ lifts to a one-to-one map of the flow region G onto the Riemann surface $\mathfrak{D} \subseteq \Omega$, having a single first order branch point over $z = \infty$. The correspondence is a homeomorphism, and in fact a conformal map between Riemann surfaces.

4. - The integrated stream function.

The domain of the stream function $\psi(z)$ is the flow region G , which is in one-to-one correspondence with the hodograph domain \mathfrak{D} . By restricting ψ to the \mathfrak{D}_+ and \mathfrak{D}_- sheets of \mathfrak{D} , we obtain two functions of (θ, σ) :

$$\psi_+(\theta, \sigma) = \psi(z), \quad z \in G_+$$

and

$$\psi_-(\theta, \sigma) = \psi(z), \quad z \in G_-,$$

where

$$\theta + i\sigma = -i \log \overline{V(z)}.$$

Recall that $\psi(z)$ is harmonic on G . Since the transformation from z to $\theta + i\sigma$ is anticonformal, ψ_+ and ψ_- are harmonic on \mathfrak{D}_+ and \mathfrak{D}_- respectively. Further, since \mathfrak{D}_+ and \mathfrak{D}_- are bounded by $C^{1,\alpha}$ curves $\sigma = l_+(\theta)$ and $\sigma = l_-(\theta)$, ψ_+ and ψ_- are of class $C^{1,\alpha}$ up to their respective boundaries.

Γ_+ and Γ_- . In fact, since the Γ_+ and Γ_- boundaries in \mathcal{D}_+ and \mathcal{D}_- correspond to the profile boundary ∂G in physical coordinates, it is clear from (2.3) that ψ_+ and ψ_- vanish on Γ_+ and Γ_- respectively.

In analogy with Brezis and Stampacchia [1], we introduce the integrated stream functions

$$(4.1) \quad \left\{ \begin{array}{l} \mathfrak{U}_+(\theta, \sigma) = e^{-\sigma} \int_{l_+(\theta)}^{\sigma} e^s \psi_+(\theta, s) ds, \quad (\theta, \sigma) \in \mathcal{D}_+ \\ \mathfrak{U}_-(\theta, \sigma) = e^{-\sigma} \int_{l_-(\theta)}^{\sigma} e^s \psi_-(\theta, s) ds, \quad (\theta, \sigma) \in \mathcal{D}_-. \end{array} \right.$$

Note that the functions \mathfrak{U}_{\pm} are not defined on the cut lines, nor at the branch point. These functions compositly define a function \mathfrak{U} on the subset $\mathcal{D}_+ \cup \mathcal{D}_- \subseteq \mathcal{D}$. However, \mathfrak{U} is not continuous across the cut lines γ_A and γ_B . In the case of a symmetric profile, Brezis and Stampacchia [1] show that \mathfrak{U}_+ can be extended to a continuous function on \mathcal{D}_+ , and so is continuous «jumping the cut» (from the left shore of the cut on \mathcal{D}_+ to the right shore on \mathcal{D}_+). This is no longer true in the nonsymmetric case, but of little consequence. We will eventually show that \mathfrak{U} is the solution to a variational inequality whose admissible functions are defined on the Riemann surface Ω and have specified jumps across the cuts γ_A and γ_B . The curves Γ_+ and Γ_- will arise as the free boundaries of the solution.

When \mathcal{D}_{\pm} and \mathfrak{U}_{\pm} are constructed in the case of a symmetric profile, one finds that the curves Γ_{\pm} are identical, that the two sheets are the same, and that $\mathfrak{U}_-(\theta, \sigma) = -\mathfrak{U}_+(\theta, \sigma)$. When the profile is nonsymmetric, both sheets play a role in determining the function \mathfrak{U} . Nonetheless, many of the results of Section 4 of [1] carry over. For example:

THEOREM 4.1. *\mathfrak{U}_+ and \mathfrak{U}_- solve the Cauchy problems*

$$(4.2) \quad \frac{\partial \mathfrak{U}_{\pm}}{\partial \sigma} + \mathfrak{U}_{\pm} = \psi_{\pm} \text{ in } \mathcal{D}_{\pm}, \quad \mathfrak{U}_{\pm}(\theta, l_{\pm}(\theta)) = 0 \quad (1).$$

Further,

$$(4.3) \quad \mathfrak{U}_{\pm}(\theta, \sigma) = \bar{\psi}(z) - e^{-\sigma} S_{\pm}(\theta)$$

(1) The two Cauchy problems are obtained by choosing the + subscript or the - subscript consistently in all occurrences. This convention of writing pairs of equations simultaneously is used throughout.

where

$$(4.4) \quad \begin{cases} \bar{\psi}(z) = \psi(z) - x \frac{\partial \psi}{\partial x}(z) - y \frac{\partial \psi}{\partial y}(z), \\ z = x + iy \in G_{\pm}, \quad \theta + i\sigma = -i \log \overline{V(z)}, \end{cases}$$

and

$$(4.5) \quad S_{\pm}(\theta) = (X_{\pm}(\theta) \sin \theta - Y_{\pm}(\theta) \cos \theta).$$

PROOF. The first statement follows from a simple computation of $\partial \mathcal{U}_{\pm} / \partial \sigma$ from (4.1). The second representation follows in an identical manner to the proof of Theorem 4.1 of [1], or alternatively to the proof of Theorem VII.8.2 of [7].

LEMMA 4.2. *The functions \mathcal{U}_{\pm} are $C^{2,\alpha}$ on $\mathcal{D}_{\pm} \cup \Gamma_{\pm}$ respectively, and satisfy*

$$(4.6) \quad -\Delta \mathcal{U}_{\pm} = e^{-\sigma} R_{\pm}(\theta) \quad \text{on } \mathcal{D}_{\pm}.$$

PROOF. The proof of Theorem 4.2 of [1] applies, using the representation (4.3) above.

We next investigate the boundary behavior of \mathcal{U} . We have from (4.1),

$$(4.7) \quad \mathcal{U}_{\pm} = 0 \quad \text{on } \Gamma_{\pm}, \quad \text{and} \quad \text{grad } \mathcal{U}_{\pm} = 0 \quad \text{on } \Gamma_{\pm}.$$

Across the cut lines γ_A and γ_B , \mathcal{U} has known jumps. These conditions are generalizations of the condition on \mathcal{U}_+ along the slit line that is used in the symmetric case, but is complicated by the presence of two inequivalent sheets. There are two cut lines, and so two pairs of «shores». We define the following trace operators on each of those shores:

For $\sigma > \sigma_{\infty}$, g_+ any function defined on \mathcal{D}_+ , and g_- defined on \mathcal{D}_- , define

$$g_{\pm}(0^-, \sigma) = \lim_{\substack{(\theta, s) \rightarrow (0, \sigma) \\ \theta < 0}} g_{\pm}(\theta, s),$$

$$g_{\pm}(0^+, \sigma) = \lim_{\substack{(\theta, s) \rightarrow (0, \sigma) \\ \theta > 0}} g_{\pm}(\theta, s).$$

These traces will exist as classical limits if g_+ and g_- are sufficiently regular, and will yield functions in L^2 if g_{\pm} is only locally H^1 in \mathcal{D}_{\pm} . We may then

define

$$[[g]]_{\gamma_A}(\sigma) = g_+(0^-, \sigma) - g_-(0^+, \sigma)$$

$$[[g]]_{\gamma_B}(\sigma) = g_+(0^+, \sigma) - g_-(0^-, \sigma),$$

for any function g defined on $\mathcal{D}_+ \cup \mathcal{D}_-$, where g_{\pm} is g restricted to \mathcal{D}_{\pm} . (Recall that γ_A is the identification of the left shore of the cut on \mathcal{D}_+ with the right shore on \mathcal{D}_- , while γ_B is the other pair of shores identified).

LEMMA 4.3.

$$(4.8) \quad [[\mathfrak{U}]]_{\gamma_A}(\sigma) = [[\mathfrak{U}]]_{\gamma_B}(\sigma) = He^{-\sigma}, \quad \sigma > \sigma_{\infty}$$

$$(4.9) \quad \left[\left[\frac{\partial \mathfrak{U}}{\partial \theta} \right] \right]_{\gamma_A}(\sigma) = \left[\left[\frac{\partial \mathfrak{U}}{\partial \theta} \right] \right]_{\gamma_B}(\sigma) = -We^{-\sigma}, \quad \sigma > \sigma_{\infty}$$

where H and W are the constants defined in (2.7) and (2.8).

PROOF. We use the representation (4.3) to obtain

$$\mathfrak{U}_{\pm}(\theta, \sigma) = \tilde{\psi}(z) - e^{-\sigma}(X_{\pm}(\theta) \sin \theta - Y_{\pm}(\theta) \cos \theta),$$

$$\frac{\partial \mathfrak{U}_{\pm}}{\partial \theta}(\theta, \sigma) = \frac{\partial}{\partial \theta} \tilde{\psi}(z) - e^{-\sigma}(X_{\pm}(\theta) \cos \theta + Y_{\pm}(\theta) \sin \theta).$$

(Note that Equation (2.6) is used in the calculation of $\partial \mathfrak{U}_{\pm} / \partial \theta$.) Since $\tilde{\psi}(z)$, defined in (4.4), is smooth on G (harmonic, in fact), it contributes no jump along the slits γ_A and γ_B on the corresponding Riemann surface \mathcal{D} . Likewise, $\partial \tilde{\psi} / \partial \theta$ has no jumps. The result follows by evaluating the jumps in the remaining terms from the \mathcal{D}_- to \mathcal{D}_+ sheet along the shores of the cuts $\theta = 0, \sigma \geq \sigma_{\infty}$.

We note that only condition (4.8) will be used to specify the boundary behavior of the class of competing functions. The remaining conditions (4.9) and (4.7) will be used to derive the variational inequality. We will also need:

LEMMA 4.4. $\mathfrak{U}_+ \in H^1(\mathcal{D}_+)$ and $\mathfrak{U}_- \in H^1(\mathcal{D}_-)$.

PROOF. The proof given by Brezis and Stampacchia of Lemma 4.5 carries over with minor modifications, providing one shows that $\mathfrak{U}_{\pm}(\theta, \sigma)$ decays like $e^{-\sigma}$ as $\sigma \rightarrow +\infty$. This fact can be established from (4.3) rewritten as

$$e^{\sigma} \mathfrak{U}_{\pm}(\theta, \sigma) = e^{\sigma} \psi(z) + x \sin \theta - y \cos \theta - S_{\pm}(\theta).$$

It suffices to show that $e^\sigma \psi(z)$ vanishes as $\sigma \rightarrow +\infty$ along any vertical line (θ, σ) on either sheet, for then $e^\sigma \mathcal{U}_\pm(\theta, \sigma)$ remains bounded as $\sigma \rightarrow +\infty$. Fix θ , and consider the vertical line (θ, s) , $s \rightarrow \infty$ in either \mathcal{D}_+ or \mathcal{D}_- : The line corresponds to a path in G , which we denote by $z(s) = x(s) + iy(s)$. Recalling that z_A and z_B are the stagnation points (equation (3.3)), we have

$$\lim_{s \rightarrow \infty} z(s) = z_A \quad \text{or} \quad z_B.$$

Since $\psi(z_A) = \psi(z_B) = 0$,

$$\begin{aligned} |\psi(z(\sigma))| &= \left| -\int_\sigma^\infty \frac{\partial \psi}{\partial x}(z(s)) \cdot \frac{\partial x}{\partial s}(s) + \frac{\partial \psi}{\partial y}(z(s)) \cdot \frac{\partial y}{\partial s}(s) ds \right| = \\ &= \left| \int_\sigma^\infty -q_2 \frac{\partial x}{\partial s} + q_1 \frac{\partial y}{\partial s} ds \right| \leq \sup_{s \geq \sigma} |V(z(s))| \cdot l(\sigma) = e^{-\sigma} l(\sigma), \end{aligned}$$

where $l(\sigma)$ is the arclength of $z(s)$ from $s = \sigma$ to $s = \infty$. Since $l(\sigma) \rightarrow 0$ as $\sigma \rightarrow \infty$, the result follows.

We extend the composite function \mathcal{U} defined on $\mathcal{D}_+ \cup \mathcal{D}_-$ to the domain $\Omega_+ \cup \Omega_-$, by setting $\mathcal{U} = 0$ on $(\Omega_+ \cup \Omega_-) \setminus (\mathcal{D}_+ \cup \mathcal{D}_-)$ ⁽²⁾. Since \mathcal{U}_\pm and $\text{grad } \mathcal{U}_\pm$ vanish on Γ_\pm (equation (4.7)), the extended functions \mathcal{U}_\pm are in $H^1(\Omega_\pm)$.

At this point, we have established all but one of the necessary properties in order to pose \mathcal{U} as the solution to a variational inequality. In the symmetric case, it is evident from the definition of \mathcal{U}_+ that $\mathcal{U}_+ \geq 0$ (see Proposition 1.1 of [1]). One might suppose the validity of

$$(4.10) \quad \begin{cases} \mathcal{U}_+ \geq 0 & \text{on } \Omega_+ \\ \mathcal{U}_- \leq 0 & \text{on } \Omega_- \end{cases}$$

in the convex nonsymmetric case, which would follow trivially if it were true that $\psi(z) \geq 0$ on G_+ and $\psi(z) \leq 0$ on G_- . However, the latter inequalities are in general false. Nonetheless, we will show in Section 5 that the inequalities (4.10) are true.

5. – The variational inequality.

In this section, we show that the integrated stream function \mathcal{U} defined on the two sheets of the Riemann surface Ω , as defined in Section 4, satis-

⁽²⁾ All unions are taken as disjoint unions in the Riemann surface Ω .

fies a variational inequality. Theorem 5.3 establishes the inequalities (4.10), which allow us to state and prove the variational inequality for \mathfrak{U} in Theorem 5.4. The first lemma, which is needed for Theorem 5.3, shows that once \mathfrak{U} is obtained as the solution to a variational inequality, the flow solution $\bar{q}(z)$ solving (2.1) may be determined quite easily.

LEMMA 5.1. *Let $q_1 + iq_2 = e^{i\theta - \sigma}$ be coordinates on Ω_+ and Ω_- . Then*

$$(5.1) \quad \left(\frac{\partial}{\partial q_2} - i \frac{\partial}{\partial q_1} \right) \mathfrak{U}_{\pm}(\theta, \sigma) = (x - X_{\pm}(\theta)) + i(y - Y_{\pm}(\theta)),$$

where $z = x + iy \in G_{\pm}$ is the point corresponding to $\theta + i\sigma \in \mathfrak{D}_{\pm}$ by the hodograph map $\theta + i\sigma = -i \log \bar{V}(z)$.

PROOF. We use the representation (4.3)

$$\mathfrak{U}_{\pm}(\theta, \sigma) = \bar{\psi}(z) - e^{-\sigma} S_{\pm}(\theta),$$

where $z \in G_{\pm}$ is the point corresponding to $\theta + i\sigma \in \mathfrak{D}_{\pm}$. Here $\bar{\psi}(z)$ is the negative of the Legendre transform of ψ , given by (4.4), and $S_{\pm}(\theta)$ is defined by (4.5). A simple computation, using (2.4), shows that for $z = x + iy$,

$$(5.2) \quad \frac{\partial \bar{\psi}}{\partial q_1}(z) = -y, \quad \frac{\partial \bar{\psi}}{\partial q_2}(z) = x,$$

expressing part of the duality of the Legendre transform. Another calculation, using (2.6), shows

$$(5.3) \quad \left(\frac{\partial}{\partial q_2} - i \frac{\partial}{\partial q_1} \right) e^{-\sigma} S_{\pm}(\theta) = X_{\pm}(\theta) + iY_{\pm}(\theta).$$

Equation (5.1) follows immediately from (5.2) and (5.3).

The practical consequence of Lemma 5.1 is that the function \mathfrak{U} allows one to assign flow velocities to physical points, thereby constructing the flow solution $\bar{q}(z)$. However, the following corollary will be needed for Theorem 5.3.

COROLLARY 5.2. *\mathfrak{U} cannot attain an interior maximum or minimum in \mathfrak{D}_+ or \mathfrak{D}_- .*

PROOF. At an interior maximum or minimum, $\text{grad } \mathfrak{U} = 0$. Suppose, for example, that an extremum occurs at the point (θ_0, σ_0) of \mathfrak{D}_+ . Since

the (q_1, q_2) coordinates are conformally related to the (θ, σ) coordinates, we have

$$\frac{\partial \mathfrak{U}_+}{\partial q_1}(\theta_0, \sigma_0) = \frac{\partial \mathfrak{U}_+}{\partial q_2}(\theta_0, \sigma_0) = 0.$$

Thus, according to (5.1), the point $z = x + iy \in G_+$ corresponding to $\theta_0 + i\sigma_0 \in \mathfrak{D}_+$ is

$$x + iy = X_+(\theta_0) + iY_+(\theta_0) \in \partial \mathfrak{F}.$$

But the hodograph map of G_+ onto \mathfrak{D}_+ given by $-i \log \overline{V(z)}$ is a homeomorphism, so the interior point (θ_0, σ_0) cannot be mapped to a boundary point. The corollary follows.

In the symmetric profile case, the following theorem is a triviality. For the more general case, we must use many of the special properties of \mathfrak{U} in order to prove:

THEOREM 5.3. $\mathfrak{U}_+ \geq 0$ on Ω_+ and $\mathfrak{U}_- \leq 0$ on Ω_- .

PROOF. We will first show that $\mathfrak{U}_+ \geq 0$ along both shores of the slit in Ω_+ , and $\mathfrak{U}_- \leq 0$ along both shores of the slit in Ω_- .

Consider the function

$$(5.4) \quad w(z) = \psi(z) - q_\infty \cdot y, \quad \text{for } z = x + iy \in G.$$

Since $w(z) = \text{Im}[\Phi(z) - q_\infty z]$, where $\Phi(z)$ is the complex potential defined by (2.2), $w(z)$ is harmonic in G . Near $z = \infty$, we have the expansions

$$V(z) = q_\infty + \frac{a_2}{z^2} + \dots, \quad \Phi(z) = q_\infty z + a_0 - \frac{a_2}{z} + \dots$$

Note that conditions 2.1 (iv) and (vi) imply that the $1/z$ term for $V(z)$ vanishes, so that $\Phi(z)$ has no $\log z$ term. Clearly, $\Phi(z) - q_\infty z$ is bounded in G , so $w(z)$ is a bounded harmonic function defined on $G \cup \{\infty\}$.

Applying the maximum principle, we know that $w(z)$ attains its maximum and minimum on $\partial \mathfrak{F}$. Since $Y_-(0) \leq y \leq Y_+(0)$ for $x + iy \in \partial \mathfrak{F}$, and since $\psi = 0$ on $\partial \mathfrak{F}$, we conclude that

$$(5.5) \quad -q_\infty Y_+(0) = \min_{\partial \mathfrak{F}} w \leq w(z) \leq \max_{\partial \mathfrak{F}} w = -q_\infty Y_-(0)$$

for all $z \in \overline{G} \cup \{\infty\}$.

Note that

$$\bar{\psi}(z) = \text{Im}[\Phi(z) - zV(z)],$$

so

$$w(\infty) = \lim_{|z| \rightarrow \infty} [\text{Im}\Phi(z) - q_\infty z] = \lim_{|z| \rightarrow \infty} \text{Im}[\Phi(z) - zV(z)] = \bar{\psi}(\infty).$$

Applying (5.5), we have

$$(5.6) \quad -q_\infty Y_+(0) \leq \bar{\psi}(\infty) \leq -q_\infty Y_-(0).$$

If we compute \mathfrak{U}_+ and \mathfrak{U}_- at the branch point using the formula (4.3) for \mathfrak{U} , we obtain

$$\mathfrak{U}_\pm(0, \sigma_\infty) = \bar{\psi}(\infty) - e^{-\sigma_\infty} S_\pm(0) = \bar{\psi}(\infty) + q_\infty Y_\pm(0).$$

Accordingly, (5.6) shows that $\mathfrak{U}_+ \geq 0$ and $\mathfrak{U}_- \leq 0$ at the branch point.

Further, from Lemma 4.4, we know that

$$\lim_{\sigma \rightarrow \infty} \mathfrak{U}(0^\pm, \sigma) = 0.$$

Thus if \mathfrak{U}_+ has a negative minimum on one of the two shores of the slit in Ω_+ , it must be attained at some point, say $(0^+, \sigma_0)$, with $\sigma_\infty < \sigma_0 < \infty$. At that point, we have

$$(5.7) \quad \mathfrak{U}_+(0^+, \sigma_0) < 0$$

and

$$(5.8) \quad \frac{\partial \mathfrak{U}_+}{\partial \sigma}(0^+, \sigma_0) = 0.$$

But

$$\begin{aligned} \frac{\partial \mathfrak{U}_+}{\partial \sigma} &= \frac{\partial \mathfrak{U}_+}{\partial q_1} \frac{\partial q_1}{\partial \sigma} + \frac{\partial \mathfrak{U}_+}{\partial q_2} \frac{\partial q_2}{\partial \sigma} = (y - Y_+(\theta))q_1 - (x - X_+(\theta))q_2 = \\ &= e^{-\sigma_0}(y_0 - Y_+(0)) \end{aligned}$$

at the point $(0^+, \sigma_0)$, corresponding to $z_0 = x_0 + iy_0 \in G$. Thus (5.8) implies that $y_0 = Y_+(0)$, so

$$w(z_0) = \psi(z_0) - q_\infty y_0 = \psi(z_0) - q_\infty Y_+(0).$$

But since $-q_\infty Y_+(0) \leq w(z_0)$ by (5.5), we have

$$(5.9) \quad \psi(z_0) \geq 0.$$

Formula (4.2) for \mathfrak{U} implies that

$$\frac{\partial \mathfrak{U}_\pm}{\partial \sigma}(0^+, \sigma_0) + \mathfrak{U}_\pm(0^+, \sigma_0) = \psi(z_0),$$

so (5.8) and (5.9) yield $\mathfrak{U}_+(0^+, \sigma_0) = \psi(z_0) \geq 0$. This contradicts (5.7), and so \mathfrak{U}_+ cannot have a negative minimum along either shore of the slit.

In a similar fashion, one can show that \mathfrak{U}_- cannot have a positive maximum along either shore of the Ω_- slit. We have shown that

$$\begin{aligned} \mathfrak{U}_+(0^\pm, \sigma) &\geq 0, & \sigma_\infty &\leq \sigma \\ \mathfrak{U}_-(0^\pm, \sigma) &\leq 0, & \sigma_\infty &\leq \sigma. \end{aligned}$$

In addition, $\mathfrak{U}_\pm = 0$ on Γ_\pm , so

$$(5.10) \quad \begin{aligned} \mathfrak{U}_+ &\geq 0 && \text{on } \partial \mathfrak{D}_+ \\ \mathfrak{U}_- &\leq 0 && \text{on } \partial \mathfrak{D}_-. \end{aligned}$$

The theorem follows by applying Corollary 5.2.

The main result is the variational inequality which follows. We will use the convention $\iint_{\Omega_+ \cup \Omega_-} g \, d\theta \, d\sigma = \iint_{\Omega_+} g_+ \, d\theta \, d\sigma + \iint_{\Omega_-} g_- \, d\theta \, d\sigma$, for any function g defined on $\Omega_+ \cup \Omega_-$. Recall that the constants H and W are defined by (2.7) and (2.8), and $R(\theta)$ is defined on $\Omega_+ \cup \Omega_-$ by the formula (2.9).

THEOREM 5.4. *Define*

$\mathbf{K} = \{V \text{ defined on } \Omega_+ \cup \Omega_-, V = V_+ \text{ on } \Omega_+, V = V_- \text{ on } \Omega_- \text{ such that}$

- $$(5.11) \quad \begin{aligned} \text{(i)} \quad &V_\pm \in H^1(\Omega_\pm); \\ \text{(ii)} \quad &[[V]]_{\gamma_A}(\sigma) = [[V]]_{\gamma_B}(\sigma) = H \cdot e^{-\sigma}, \quad \sigma > \sigma_\infty; \\ \text{(iii)} \quad &V_\pm(-\pi, \sigma) = V_\pm(\pi, \sigma) = 0, \text{ for all } \sigma; \\ \text{(iv)} \quad &V_+ \geq 0 \text{ on } \Omega_+, \text{ and} \\ \text{(v)} \quad &V_- \leq 0 \text{ on } \Omega_-. \end{aligned}$$

Then the integrated stream function \mathcal{U} defined in section 4 satisfies $\mathcal{U} \in \mathbf{K}$, and for all $\mathcal{V} \in \mathbf{K}$,

$$(5.12) \quad \iint_{\Omega_+ \cup \Omega_-} \text{grad } \mathcal{U} \cdot \text{grad } (\mathcal{V} - \mathcal{U}) \, d\theta \, d\sigma \geq \iint_{\Omega_+ \cup \Omega_-} R(\theta) e^{-\sigma} (\mathcal{V} - \mathcal{U}) \, d\theta \, d\sigma - \int_{\gamma_A} W e^{-\sigma} (\mathcal{V}_+ - \mathcal{U}_+)(0^-, \sigma) \, d\sigma + \int_{\gamma_B} W e^{-\sigma} (\mathcal{V}_+ - \mathcal{U}_+)(0^+, \sigma) \, d\sigma.$$

PROOF. Lemmas 4.4 and 4.3 show that \mathcal{U} satisfies (i) and (ii) of the definition of \mathbf{K} . Condition (iii) follows since $\mathcal{U} = 0$ on $\Omega \setminus \mathcal{D}$, and (iv) and (v) are given by Theorem 5.3, to show that $\mathcal{U} \in \mathbf{K}$.

Next, we wish to *formally* integrate the left side of (5.12) by parts. The integrand is nonzero outside $\mathcal{D}_+ \cup \mathcal{D}_-$, so applying Lemma 4.2, the integral becomes

$$(5.13) \quad \iint_{\mathcal{D}_+ \cup \mathcal{D}_-} \text{grad } \mathcal{U} \cdot \text{grad } (\mathcal{V} - \mathcal{U}) \, d\theta \, d\sigma = \iint_{\mathcal{D}_+ \cup \mathcal{D}_-} R(\theta) e^{-\sigma} \cdot (\mathcal{V} - \mathcal{U}) \, d\theta \, d\sigma + \int_{\partial \mathcal{D}_+ \cup \partial \mathcal{D}_-} (\text{grad } \mathcal{U} \cdot \bar{n}) \cdot (\mathcal{V} - \mathcal{U}) \, dl,$$

where \bar{n} is the outward normal vector. The boundary terms in (5.13) vanish on I_{\pm} according to (4.7). Along the slits, $\text{grad } \mathcal{U} \cdot \bar{n} = (\partial \mathcal{U} / \partial \theta)(0^-, \sigma)$ on the left shores, and $-(\partial \mathcal{U} / \partial \theta)(0^+, \sigma)$ on the right shores. Note that $\mathcal{V} - \mathcal{U}$ is defined on the slits because \mathcal{V} and \mathcal{U} have equal jumps. Applying Lemma 4.3, the final term in (5.13) gives rise to the final two terms in (5.12).

Since $\mathcal{U} = 0$ on $\Omega \setminus \mathcal{D}$ and since $\mathcal{V} \in \mathbf{K}$, $\mathcal{V}_+ - \mathcal{U}_+ \geq 0$ on $\Omega_+ \setminus \mathcal{D}_+$, and $\mathcal{V}_- - \mathcal{U}_- \leq 0$ on $\Omega_- \setminus \mathcal{D}_-$. Applying (2.10), we see that

$$\iint_{\Omega \setminus \mathcal{D}} R(\theta) e^{-\sigma} (\mathcal{V} - \mathcal{U}) \, d\theta \, d\sigma \leq 0.$$

Accordingly, the integral (5.13) is greater than or equal to the right-hand side of (5.12), thus justifying (5.12) by a formal integration by parts.

To make the formal calculation above more precise, one must consider the singularity in $\text{grad } \mathcal{U}$ at the branch point, and convergence on both sheets as $\sigma \rightarrow +\infty$. The method used in Theorem 4.6 of [1] carries over to the two sheeted surface to show that the formal calculation above is valid.

Since the variational inequality (5.11), (5.12) will have a unique, regular solution [8, 9], the integrated stream function \mathcal{U} can be obtained by solving the variational inequality.

6. – Remarks.

We have shown that the function \mathcal{U} is the solution to the variational inequality (5.12), and that the solution $\bar{q} = (q_1, q_2)$ to Problem (2.1) can be obtained from \mathcal{U} by means of Lemma 5.1. The resulting representation of the solution provides an inverse map of the multi-sheeted hodograph domain onto the physical plane. For this reason, in a practical implementation of these results, the solution automatically provides a dynamic quantization of the flow region. For example, if the hodograph domain is quantized by a uniform grid, the physical domain will be finely quantized in those areas where the flow velocity changes rapidly, and more coarsely quantized in those regions where the flow is nearly uniform.

The variational inequality (5.12) has been viewed as a relation for a function \mathcal{U} which is defined on a naturally occurring Riemann surface. It is possible to unfold the Riemann surface Ω by means of a $\sqrt{\theta + i\sigma - i\sigma_\infty}$ transformation and reformulate (5.12) as a variational inequality whose competing functions are defined on a new domain $\tilde{\Omega} \subset \mathbb{C}$. Such a process offers no advantage over the more natural representation of Ω as a Riemann surface.

Since the two sheets of Ω , namely Ω_+ and Ω_- , are identical, it is possible to consider \mathcal{U}_+ and \mathcal{U}_- as functions of a single strip domain, and reformulate the variational inequality as a variational system, with a coupling between \mathcal{U}_+ and \mathcal{U}_- given by the jump conditions. This observation is useful for numerical implementation.

Analogs of Theorems 5.1 and 5.2 of [1] carry over, but are omitted here. We note however that one of the principal advantages of the method of solution described here is that the solution domain, the hodograph domain, is essentially compact. Indeed, a lower bound for σ can be obtained a-priori, and since the distributions in the variational inequality are weighted by $e^{-\sigma}$, there is little lost if one truncates Ω for sufficiently large σ .

REFERENCES

- [1] H. BREZIS - G. STAMPACCHIA, *The hodograph method in fluid-dynamics in the light of variational inequalities*, Arch. Rational Mech. Anal., **61** (1976), pp. 1-18.
- [2] G. STAMPACCHIA, *Le disequazioni variazionali nella dinamica dei fluidi. Metodi valutativi della Fisica-Matematica*, Accad. Naz. Lincei, Quaderno n. 217 (1975). pp. 169-180.

- [3] F. TOMARELLI, *Un problème de fluidodynamique avec les inéquations variationnelles*, C. R. Acad. Sci. Paris, **286** (1978), pp. 999-1002.
- [4] H. BREZIS - G. DUVANT, *Écoulement avec sillage autour d'un profilé symétrique sans incidence*, C. R. Acad. Sci. Paris, **276** (1973), pp. 875-878.
- [5] W. RUDIN, *Real and Complex Analysis*, McGraw Hill, 1966.
- [6] S. WARSCHAWSKI, *On differentiability at the boundary in conformal mapping*, Proc. Amer. Math. Soc., **12** (1961), pp. 614-620.
- [7] D. KINDERLEHRER - G. STAMPACCHIA, *An Introduction to Variational Inequalities and their Applications*, Academic Press, 1980.
- [8] H. LEWY - G. STAMPACCHIA, *On the regularity of the solution of a variational inequality*, Comm. Pure Appl. Math., **22** (1969), pp. 153-188.
- [9] J. L. LIONS - G. STAMPACCHIA, *Variational inequalities*, Comm. Pure Appl. Math., **20** (1967), pp. 493-519.

Courant Institute of Mathematical Sciences
New York University
251 Mercer Street
New York, N. Y. 10012